



Research article

Cradle to Gate LCA analysis for wrought aluminum recycling process from high impurity content alloys with the fractional crystallization technology

Kotaro Kawajiri ¹, Michio Kobayashi ¹ and Yuichiro Murakami ²

¹ AIZOTH. Inc 2nd Floor, Daiwa Roynet Hotel Tsukuba Bldg, 1-5-7 Azuma, Tsukuba, IBARAKI 305-0031, Japan

² National Institute of Advanced Industrial Science and Technology, Chubu center, Multi material research section, Light metal process group, 205, Sakurazaka 4 chome, Moriyama city, Aichi prefecture, 436-8560, Japan

***Correspondence:** Email: kotaro.kawajiri@aizoth.com; Tel: +81-(50)3695-9622.

Abstract: An increasing demand for wrought aluminum, such as in the automobile field, requires the recycling of scraped aluminum into low-impurity-content wrought aluminum in an environmentally friendly manner. In this paper, the feasibility of the fractional crystallization method coupled with electromagnetic stirring (EMS) technology to obtain wrought aluminum high-quality alloys from high-impurity-content aluminum was reviewed. Also, a Cradle-to-Gate life cycle assessment (LCA) was conducted to assess the greenhouse gas (GHG) effect of this technology. Results indicate that, through this technology, the Al-rich phase was successfully separated from the impurity-rich phase. In LCA, an upscaling method was employed to assess GHG emissions. The results show that GHG emissions reduced as production scale increased. Also, GHG emissions between the lab and the pilot scales at the same production scale were compared; those extrapolated from the lab scale were notably higher. In addition, GHG emissions in an improved scenario were analyzed. At a 1,000 kg production scale, GHG emissions were 0.36 kg CO₂ eq/kg, much lower than the GHG emissions of primary aluminum (9.93 kg CO₂ eq/kg). The analysis showed that the fractional crystallization method with EMS technology is a promising technology for upgrading recycling from high-impurity cast alloys into low-impurity-content wrought aluminum alloys with very low GHG emissions.

Keywords: Recycle; fractional crystallization; wrought aluminum; LCA; Greenhouse gas (GHG); Electromagnetic stirring

1. Introduction

Aluminum is an abundant resource, and its versatility makes it extremely attractive for lightweight solutions in various industries [1]. Aluminum can be divided into two major categories regarding the concentration of alloy elements: high-purity wrought alloys have a non-aluminum content up to 10 wt%, and cast alloys, which have much higher tolerance limits, have a non-aluminum content up to 20 wt%) [2]. Cast alloys have limited applications and are mainly used in transportation, especially in the automotive sector [3]. However, the introduction of electric vehicles will result in a decrease in cast alloy demand, generating 6.1 Mt of cast alloy scrap by 2030, which cannot be recycled due to the high concentration of alloying elements [4]. Cars manufactured today have approximately 8% aluminum by weight, which is forecasted to reach 16% by the year 2028 [5]. Due to an increased use of wrought aluminum in cars, an increasing volume of wrought aluminum scrap is expected [6].

The GHG emissions of primary aluminum are 9.93 kg CO₂ eq/kg, being higher than other materials such as steel (1.83 kg CO₂ eq/kg) [7]. Aluminum recycling saves up to 95% of the energy needed to produce primary aluminum and can save GHG emissions up to 95% [6]. This is because most of the energy required to produce primary aluminum is embodied in aluminum itself and aluminum scrap. Therefore, the energy required to melt aluminum scrap is only a fraction of primary aluminum [6]; also, aluminum recycling is financially attractive as its market already exists [8].

Currently, aluminum recycling is mainly processed into cast alloys, as aluminum scrap is used where it is most efficient; currently, that corresponds to cast aluminum and not wrought aluminum [9]. Recycling into wrought aluminum remains challenging [10]. The main difficulty in producing wrought aluminum from scrap is to retain the proper chemical composition of the melt [11]. Since cast alloys have higher compositional tolerance for impurities, cast aluminum cannot be recycled into anything but cast aluminum [11]. Due to the high demand for cast aluminum, down-cycling aluminum scrap to recycle-friendly cast aluminum is a common strategy nowadays, but the future demand for cast aluminum may be different [2] due to the emergence of electric vehicles. Cullen and Allwood (2013) [12] estimated that globally, every year, 6.1 Mt of wrought aluminum scrap is downgraded into cast alloys. However, wrought alloys represent two-thirds and cast alloys represent one-third of the global aluminum demand [12]. Modaresi and Müller (2012) [9] forecasted that a continuation of the above-mentioned strategy would result in non-recyclable casting scrap surplus in 2018, with an uncertainty margin of about 5 years. Therefore, the argument arises that the amount of recycled wrought aluminum from consumer scrap should increase and be qualified for future sustainable solutions [13]. This would be an important future trend in developing new types of wrought aluminum to meet customer requirements with scrap-friendly compositions [14,15]. Therefore, with the increasing demand for wrought aluminum and its expected scrap, it is necessary to construct a sustainable system to support wrought aluminum demand by recycling it with lower GHG emissions.

The recycling technology we review in this paper is the fractional crystallization method, which is assisted by electromagnetic stirring (EMS). The fractional crystallization utilizes the phenomenon by which a molten alloy is cooled down from a liquid state to a solid state, leading to the higher-purity

metal solidifying first [16]. This method provides alloys for high-purity applications [17]. EMS accelerates the metal separation process during the fractional crystallization. EMS technology was initially introduced into the aluminum industry in the 1960s and has grown significantly since the late 1990s [18]. By using a high-intensity force field, even micrometer-sized inclusion particles can, in principle, be separated [19]. The driving force for particle motion and the direction of motion depend on the electrical conductivity difference between the metal and the inclusion particles [19]. Because the electromagnetic force induced in the molten metal is different among the inclusion particles due to their conductivity, they are forced to move along a direction opposite to the electromagnetic force and therefore can be separated from the melt [20]. This technology can be used for aluminum alloy refining. For example, in Al-Si melt under electromagnetic stirring, the primary Si phases are separated and accumulated at the periphery of the ingot during the solidification of the Al-Si melt. Eventually, a layer structure is formed with a Si-rich outer layer and an Al-rich inner layer [21]. After the aluminum ingot is separated into Al-rich and Si-rich phases, the two phases are separated by the mechanical press.

Several works have discussed upscaling techniques for different applications [22–25]. However, to our knowledge, no previous paper has analyzed predicted GHG emissions of the upscaling technique to confirm its validity with real data. In addition, in works related to EMS technology, Lee et al (2010) [26] and Murakami and Omura (2021) [27] conducted an impurity concentration analysis but did not include GHG analysis. Additionally, no LCA has been conducted for reclaimed wrought aluminum with the fractional crystallization method with EMS technology or any analysis applying the scaling technique.

Based on the above, we set the objective of this study to 1) demonstrate that the fractional crystallization method coupled with EMS can adequately separate the Al-rich phase and the Si-rich phase, 2) estimate GHG emissions of this technology based on a cradle-to-gate approach by upscaling the lab and pilot scales to the mass production scale, and 3) compare GHG emissions predicted by the lab and pilot scales and review if such predictions match GHG emissions at the mass production scale. If an analysis is conducted with the inventory data from the lab production scale, the power consumption of the equipment at the production scale is largely overestimated [25]. Therefore, its LCA at the lab scale provides misleading results. The novelty of this study is the use of real data from the lab and the pilot production scales to assess GHG emissions by the upscaling technique and to analyze whether upscaled data match predicted GHG emissions by the lab and pilot scales.

2. Methods

2.1. System boundary and functional unit

System boundary of the fractional crystallization method is shown in Figure 1.

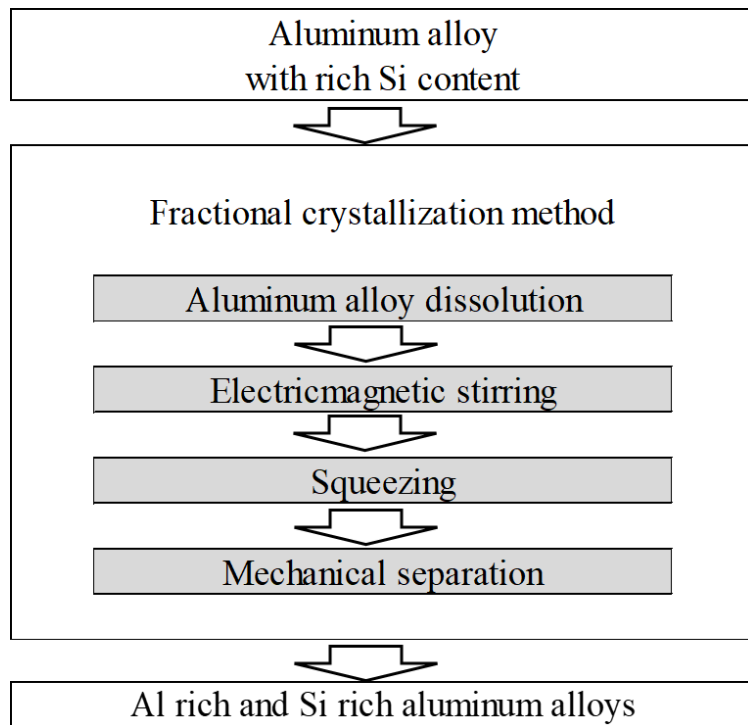


Figure 1. System boundary of the fractional crystallization process (in grey).

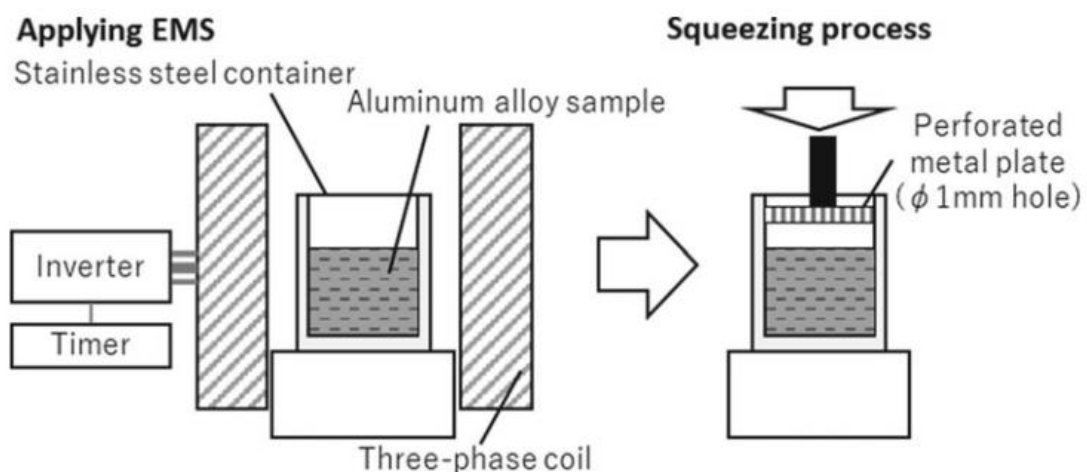


Figure 2. EMS and squeezing processes.

There are four stages to the fractional crystallization method: aluminum alloy dissolution, EMS, squeezing, and mechanical separation. Two aluminum alloys, AC4C and ADC12, were used in this study. Aluminum alloys were molten in a melting furnace for 6.0 and 2.5 h in the lab and the pilot scales at 650 °C. Molten aluminum was poured into the EMS machine and stirred. After the EMS process, solid Al-rich aluminum and molten Si-rich aluminum appeared due to the fractional crystallization effect. The molten Si-rich alloy was pressed by a perforated metal plate with a 1-mm

diameter hole using a mechanical press. The liquid state of the alloy was squeezed through the perforated metal plate. The alloy portion, which was not passed through by the perforated metal plate, was the Al-rich aluminum alloy. After cooling down, the alloy was separated by the mechanical press machine at the point of the perforated metal plate. The EMS and squeezing processes are shown in Figure 2.

The functional unit is 1 kg of reclaimed Al-rich aluminum with an impurity concentration equivalent to wrought aluminum (<10%). The final output is composed of Al-rich aluminum for wrought aluminum applications and Si-rich aluminum for cast aluminum applications. Compositional analysis of the separated alloys is performed using energy-dispersive X-ray spectroscopy (EDX).

2.2. GHG emission analysis

GHG emissions analysis is done in three steps. The first step is to analyze GHG emissions at the lab scale; lab production scale is 0.6 kg. The second step is to analyze GHG emissions at the 6.79 kg scale, which is the pilot production scale. The scaling method, which will be explained later, will be applied to assess GHG emissions at the production scale up to 10,000 kg. The third step is to compare GHG emissions predicted from the lab and pilot scales and to analyze and discuss any discrepancies. Inventory data of the lab and pilot production scales are shown in Table 1; GHG emissions were assessed based on such data.

Table 1. Inventory data of the lab and pilot production scales.

(a) Lab scale

Process		Material	Unit	Volume
Stage 1	Input	Aluminum alloy	kg	1.200
Aluminum dissolution	Energy	Electricity	kWh	16.270
	Waste	Aluminum residue	kg	0.200
	Product	Aluminum alloy	kg	1.000
Stage 2	Input	Aluminum alloy	kg	1.000
EMS	Energy	Electricity	kWh	0.140
	Waste	Aluminum residue	kg	0.000
	Product	Aluminum alloy	kg	1.000
Stage 3	Input	Aluminum alloy	kg	1.000
Squeezing	Energy	Electricity	kWh	0.000
	Waste	Aluminum residue	kg	0.000
	Product	Aluminum alloy	kg	1.000
Stage 4	Input	Aluminum alloy	kg	1.000
Mechanical separation	Energy	Electricity	kWh	0.001
	Waste	Aluminum residue	kg	0.050
	Product	Si-rich aluminum	kg	0.350
		Al-rich aluminum	kg	0.600

(b) Pilot scale

Process		Material	Unit	Volume
Stage 1	Input	Aluminum alloy	kg	30.000
Aluminum dissolution	Energy	Electricity	kWh	33.100
	Waste	Aluminum residue	kg	1.000
	Product	Aluminum alloy	kg	29.000
Stage 2	Input	Aluminum alloy	kg	10.000
EMS	Energy	Electricity	kWh	2.200
	Waste	Aluminum residue	kg	0.200
	Product	Aluminum alloy	kg	9.800
Stage 3	Input	Aluminum alloy	kg	9.800
Squeezing	Energy	Electricity	kWh	0.000
	Waste	Aluminum residue	kg	0.000
	Product	Aluminum alloy	kg	9.800
Stage 4	Input	Aluminum alloy	kg	9.800
Mechanical separation	Energy	Electricity	kWh	0.004
	Waste	Aluminum residue	kg	0.100
	Product	Si-rich aluminum	kg	2.910
		Al-rich aluminum	kg	6.790

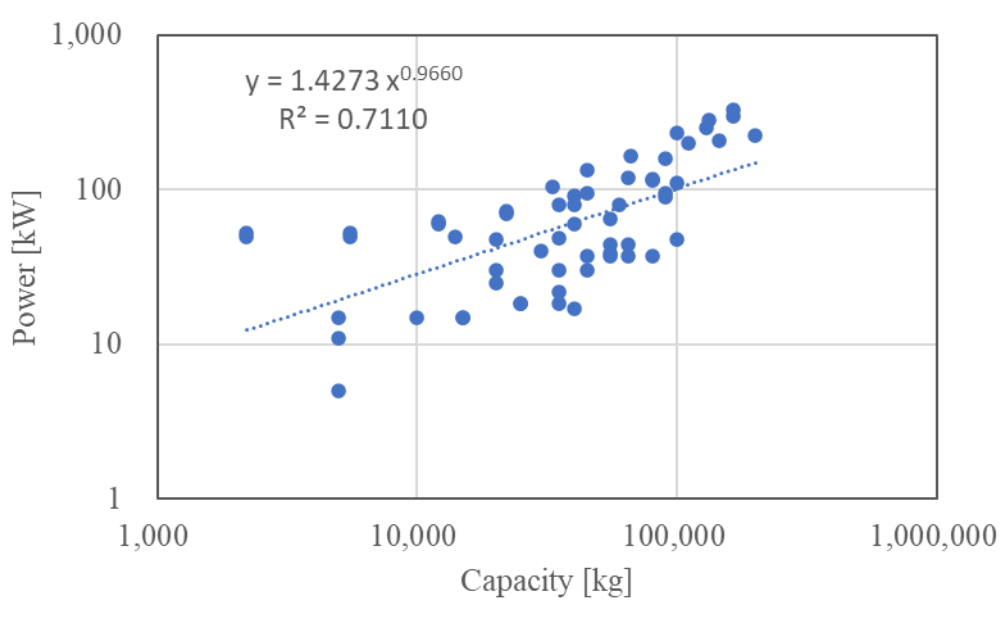
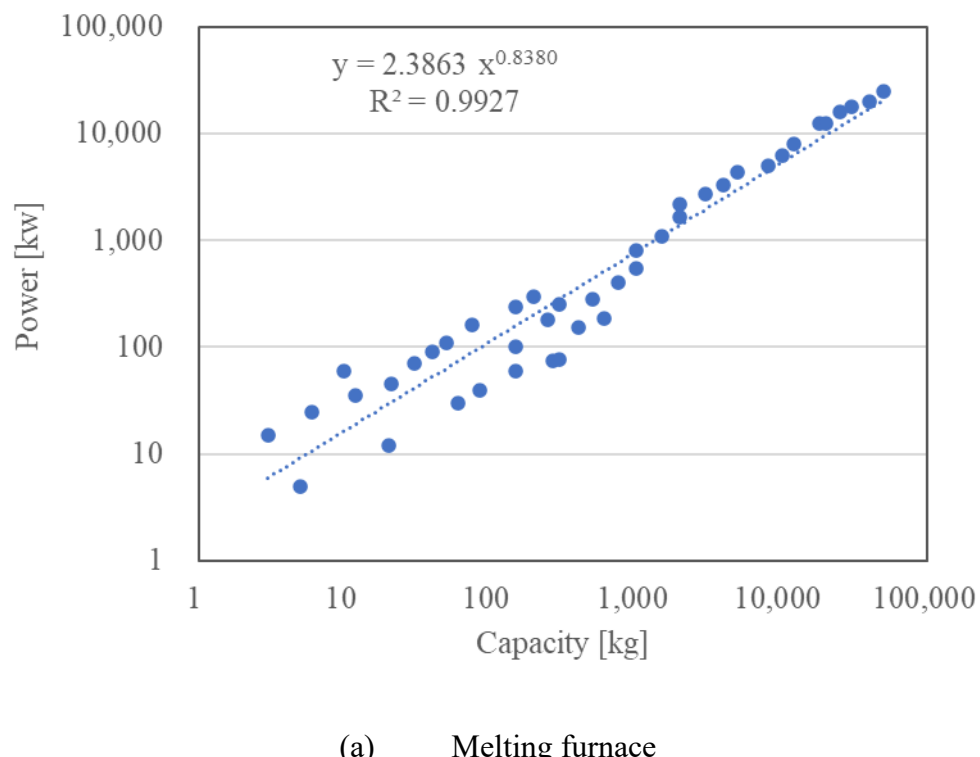
2.3. Upscaling analysis

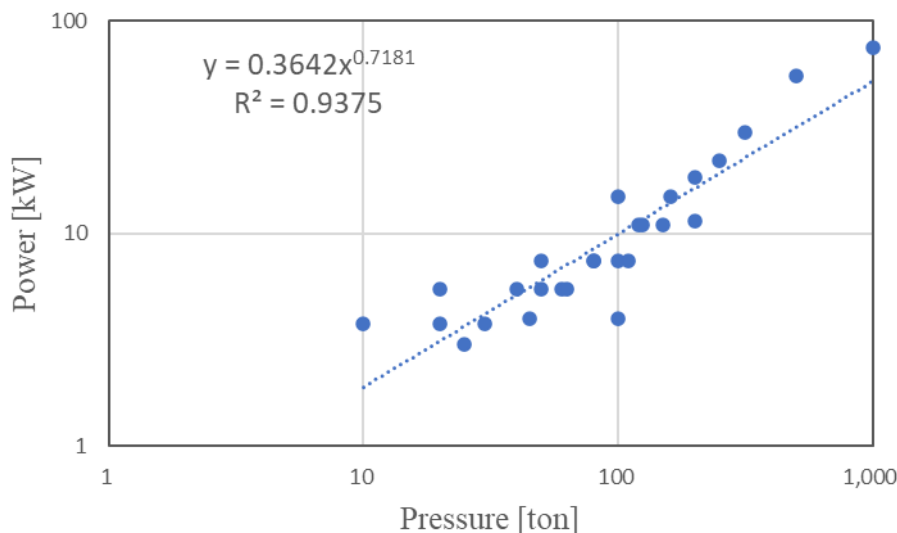
In this study, the scaling effect with changes in the production scales is introduced. Information about processing temperatures and time duration is often presented in patents and previous studies. However, information about the power consumption of each process is rarely included. Previous studies have shown that if an analysis is conducted with the inventory data from the lab scale, the power consumption of the equipment at the production scale is largely overestimated [28]. Data from the small production scale were used in the fractional crystallization method. In order to assess GHG emissions at the mass production scale, it is necessary to upscale the production scale by applying the scaling effect.

To estimate the scaling effect, we used the scale factors, which were obtained from the size and nominal power specifications of machines with different scales [21] as follows:

$$P = P_0 \left(\frac{S_x}{S_0} \right)^f \quad (1)$$

where P represents power, S is the scale of the process, f is the scale factor, subscript 0 represents the values of the lab scale, and subscript x represents the values of the target scale. The scaling factors of the melting furnace, EMS, squeezing, and mechanical press are 0.838, 0.966, 0.718, and 0.718, respectively. They are shown in Figure 3. Squeezing and mechanical presses use hydraulic press technology. Therefore, the same scale factor is assigned.





(c) Squeezing and mechanical press

Figure 3. Scaling factors of the equipment used.

In this study, in order to assess the environmental burden more precisely, GHG emissions by the equipment and the facility were taken into consideration. IDEA_v2.1.3 database [7] was used to assign GHG emissions in each category of the inventory data, as such experimental data originated in Japan, and the IDEA database was considered suitable. The GHG coefficients in the IDEA database are defined as the cost, JPY for the equipment and area, and m_2 for facilities. The calculation of the volume of the equipment includes its initial cost and its depreciation period of 7 years. The calculation of the volume of the facility includes the area of the equipment.

3. Results and discussion

3.1. Effectiveness of the fractional crystallization method with EMS technology

The material content analysis for the fractional crystallization method was conducted with AC4C and ADC12 aluminum alloys. The original impurity content for the Al-rich and impurity-rich phases is shown in Figure 4. After separation by the fractional crystallization method, the Al-rich phase of AC4C was 98.5% and the impurity-rich phase was 1.3%. As for the ADC12, the Al-rich phase was 97.6% and the impurity-rich phase was 2.4%. This analysis showed that the fractional crystallization method with EMS technology effectively separates the Al-rich phase aluminum to meet the wrought aluminum requirement of 10% or less impurity content.

3.2. GHG emissions on the lab scale

GHG emissions of the fractional crystallization method with EMS technology on the lab scale are shown in Figure 5, divided by stage and materials. GHG emissions were reduced from 30.59 kg CO₂ eq/kg at a 0.6 kg lab production scale to 6.57 kg CO₂ eq/kg at a 10,000 kg production scale. The GHG

emissions over a 0.6 kg production scale were extrapolated based on the scaling method. A reduction in GHG emissions occurred, primarily due to a reduction in electricity and an improvement in efficiency, in accordance with increasing production scales. Stage 1 occupied a majority of GHG emissions at all scales because of the processing time of the aluminum melting furnace: 6 hours to melt and mix aluminum ingot. On the other hand, GHG emissions by EMS and mechanical separation were small due to the short processing time. As for the GHG emissions by materials, electricity was the major contributor, as the GHG emissions from the melting furnace were much larger than those of any materials.

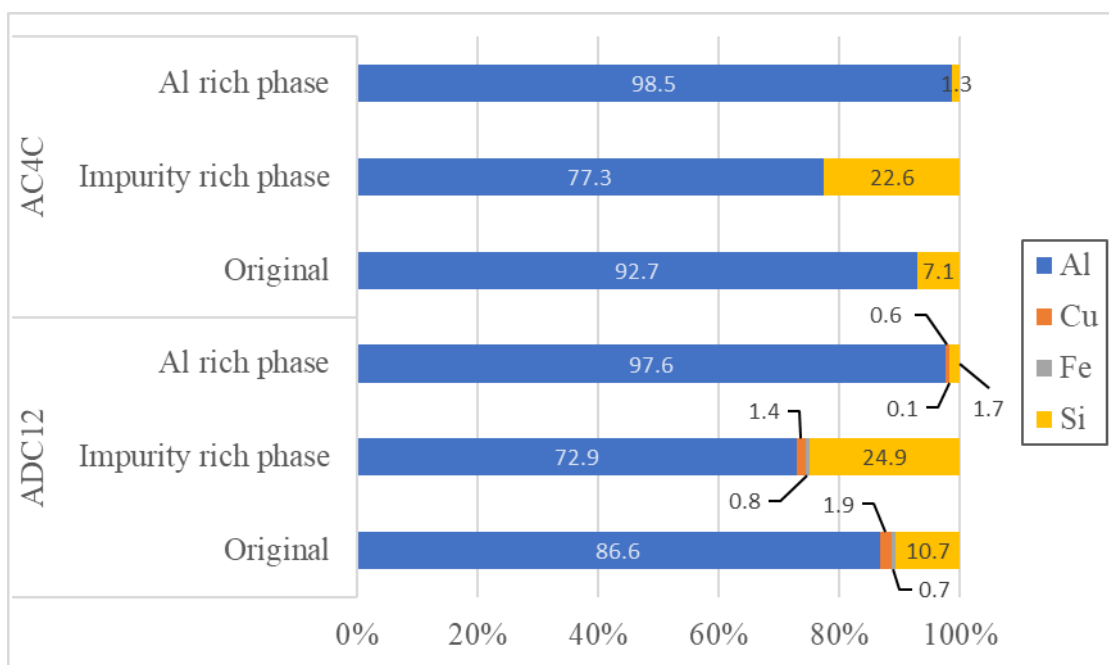
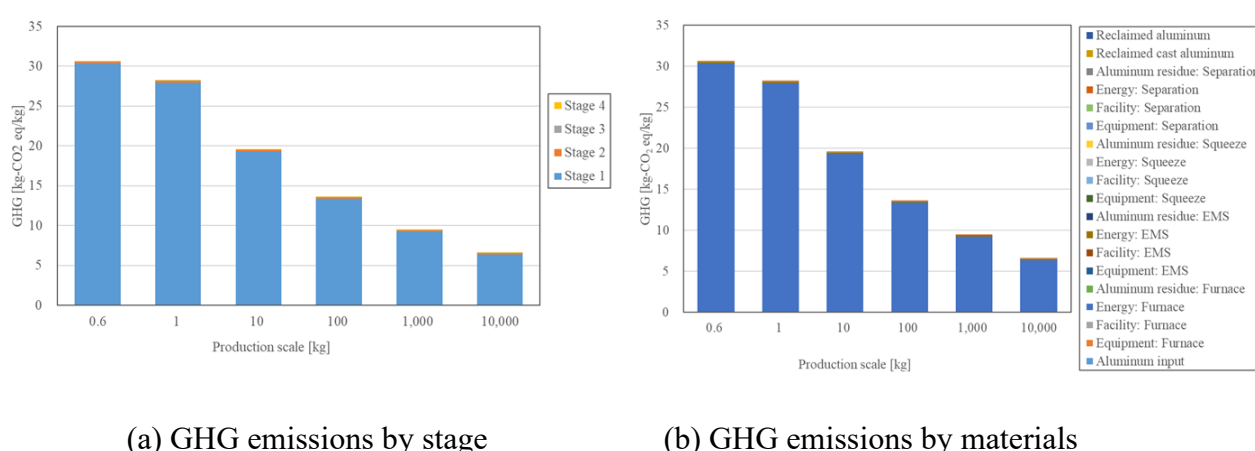


Figure 4. Impurity content analysis of AC4C and ADC12 by the fractional crystallization method with EMS technology.



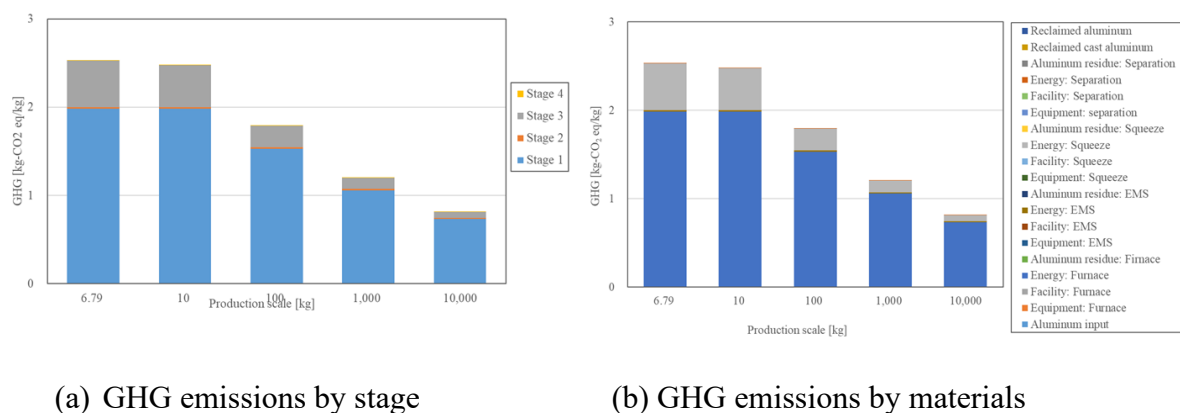
(a) GHG emissions by stage

(b) GHG emissions by materials

Figure 5. GHG emissions of the fractional crystallization process at the lab scale.

3.3. GHG emissions on the pilot scale

GHG emissions on the pilot scale are shown in Figure 6, divided by stage and materials. The pilot production scale was 6.79 kg. The values of GHG emissions over a 6.79 kg production scale were extrapolated based on the scaling method. GHG emissions at a 6.79 kg production scale were 2.53 kg CO₂ eq/kg and were reduced to 0.81 kg CO₂ eq/kg at a 10,000 kg production scale by the scaling effect. GHG emissions of Stage 1 were large because the aluminum melting furnace consumed a lot of electricity, with a processing time of 2.5 hours. As for the GHG emissions by the materials, the furnace made up 90% of the entire GHG emissions, explained by the fact that the processing time of the aluminum melting furnace was 2.5 hours, compared to those of EMS and mechanical separation, which were 0.17 and 0.02 hours, respectively.



(a) GHG emissions by stage

(b) GHG emissions by materials

Figure 6. GHG emissions of the fractional crystallization process on the pilot scale.

3.4. Comparison of GHG emissions between the lab and pilot production scales

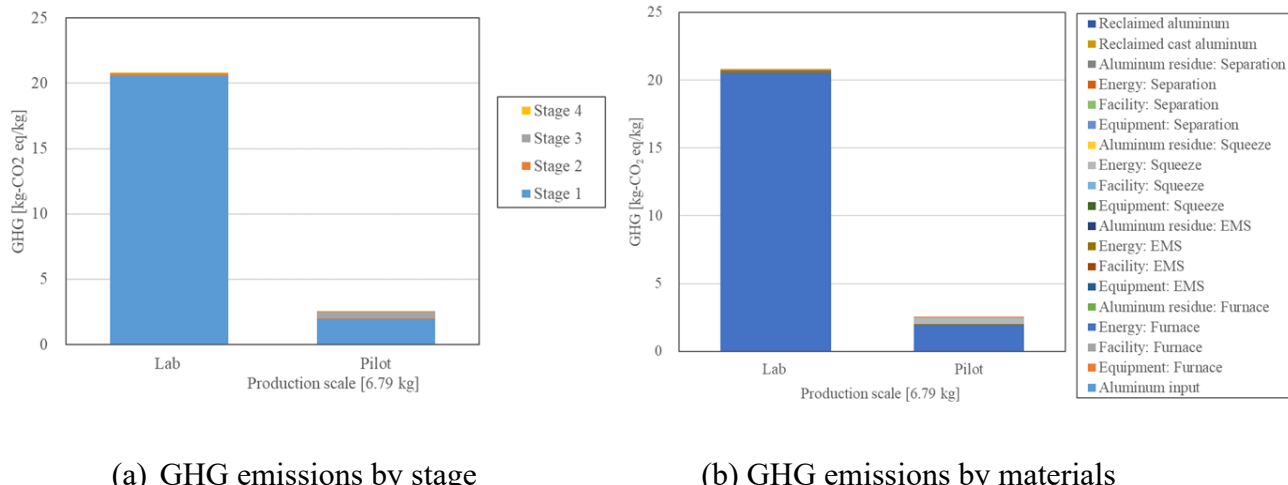
The conditions of the lab and the pilot scales are shown in Table 2. The production scale of the lab was 0.6 kg, and that of the pilot was 6.79 kg. The target production scale for GHG emissions analysis was 6.79 kg. The power consumption of each equipment, P_0 , and its processing time are also listed in Table 2. GHG emissions at a 6.79 kg production scale are shown in Figure 7. GHG emissions at a 6.79 kg production scale on the lab scale were then extrapolated. The value of the pilot scale was the real value measured at a 6.79 kg pilot production scale.

The GHG emissions on the lab and pilot scales were 20.79 and 2.53 kg CO₂ eq/kg, respectively. These values differ significantly. GHG emissions predicted based on the lab scale should be much smaller, to be close to the value of the pilot scale. GHG emissions are the function of power consumption, P , its processing time, and the scaling factor. Power consumption was upscaled from a 0.6 kg to a 6.79 kg production scale in the lab scale, while raw data was used for the pilot scale. Thus, P was not upscaled on the pilot scale. Although there were some differences in parameters such as processing time and power requirement of equipment, P_0 , the scaling effect, which was the function of the production scale ratio, $(\frac{S_p}{S_0})$, had a larger influence on GHG emissions. As a result, GHG emissions on the lab scale became much larger than those of the pilot scale. In addition, from Section

3.2 and 3.3, GHG emissions at a 10,000 kg production scale predicted from the lab scale and the pilot scale were 6.57 kg CO₂ eq/kg and 0.81 kg CO₂ eq/kg, respectively. This comparison analysis confirms our hypothesis that predicting GHG emissions at a large production scale based on a small lab production scale will lead us to an overestimated conclusion [25].

Table 2. Conditions of the lab and pilot production scales.

	Lab	Pilot
Production scale (kg)	0.60	6.79
Target output (kg)	6.79	6.79
Power consumption P_0 (kW)		
Melting furnace	5.0	25.7
EMS	2.0	1.1
Squeezing	6.0	6.0
Mechanical separation	6.0	6.0
Processing time (hour)		
Melting furnace	6.0	2.5
EMS	0.1	0.17
Squeezing	1.0	1.0
Mechanical separation	0.002	0.002



(a) GHG emissions by stage

(b) GHG emissions by materials

Figure 7. GHG emissions at a 6.79 kg production scale divided by stage and materials.

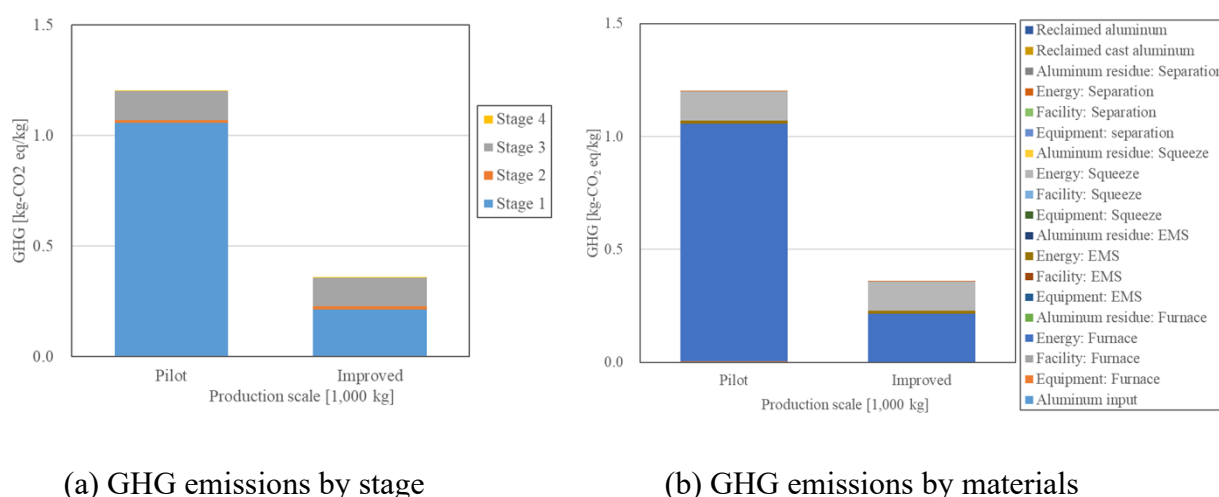
3.5. Considerations under an improved scenario

Since the duration of aluminum dissolution seems too long, we consulted the research engineer of UACJ Corporation, who designed and assembled the pilot scale plant. We learned that 2.5 hours in the pilot scale included the time to melt the aluminum alloy. In a normal production process, aluminum alloy is molten initially. However, once it is molten, additional aluminum alloy is poured into the furnace and molten quickly. The actual time for this melting process is 0.5 hours. Therefore, we

employed 0.5 hours for the aluminum melting process and did the analysis. The 1,000 kg production scale was chosen for the comparison since 1,000 kg is considered a reasonable mass production scale. The conditions of this improved scenario are shown in Table 3. The analysis was conducted based on a 6.79 kg pilot scale. The changed conditions are highlighted in gray. GHG emissions of the improved scenario are shown in Figure 8.

Table 3. Conditions of the improved scenario.

	Pilot	Improved scenario
Power consumption P_0 (kW)		
Melting furnace	25.7	25.7
EMS	1.1	1.1
Squeezing	6.0	6.0
Mechanical separation	6.0	6.0
Processing time (hour)		
Melting furnace	2.5	0.5
EMS	0.1	0.1
Squeezing	1.0	1.0
Mechanical separation	0.002	0.002



(a) GHG emissions by stage

(b) GHG emissions by materials

Figure 8. GHG emissions with improved conditions at a 1,000 kg production scale.

The GHG emissions at a 1,000 kg production scale were 1.20 kg CO₂ eq/kg with the original pilot condition and 0.36 kg CO₂ eq/kg with the improved scenario. The GHG emissions were substantially lower in the improved scenario than for the primary aluminum (9.93 kg CO₂ eq/kg) [7]. If high-impurity cast alloys are recycled, and GHG credit is given, GHG emissions under the improved scenario will be -0.14 kg CO₂ eq/kg. Thus, further improvement is expected. The fractional crystallization method successfully reclaimed wrought aluminum quality alloys in a very environmentally friendly manner.

4. Conclusions

In this paper, we reviewed the effectiveness of the fractional crystallization technology coupled with EMS technology for aluminum recycling applications and evaluated GHG emissions associated with this technology. The result indicated that this technology yielded 98.5% of Al-rich phase aluminum alloy from AC4C and 97.6% of Al-rich phase aluminum from ADC12. Therefore, this technology was proven to be effective in reclaiming high Al-rich phases that could be used in wrought aluminum applications.

An LCA was conducted using a 0.6 kg lab production scale and a 6.79 kg pilot production scale. The scaling method was applied. The results showed that GHG emissions were 6.57 kg CO₂ eq/kg at the lab scale and 0.81 kg CO₂ eq/kg at 10,000 kg production scale on the pilot scale.

Next, GHG emissions at a 6.79 kg production scale were extrapolated from the lab scale, and the 6.79 kg pilot production scale was compared. This comparison analysis confirmed our hypothesis that predicting GHG emissions at a large production scale based on a small lab production scale will lead to an overestimated conclusion.

GHG emission analysis with an improved scenario showed that GHG emissions were 0.36 kg CO₂ eq/kg, achieving a 70% reduction. Since GHG emissions of primary aluminum are 9.93 kg CO₂ eq/kg and those of a 5000 series aluminum plate are 11.2 kg CO₂ eq/kg [7], this technology proved to be very environmentally friendly and to contribute to enhancing the circular economy. In addition, further reduction in GHG emissions is expected if high-impurity cast alloys are recycled and reused.

The analysis showed that the fractional crystallization method with EMS technology is a promising approach for upgrading recycling from cast alloys with high-impurity-content into low-impurity-content wrought aluminum alloys with very low GHG emissions. However, the analysis is limited to aluminum alloys with low impurity concentration. In order to use alloys for applications such as automotive body parts, additional treatments such as rinsing and heat treatments are necessary. Future analysis should include subsequent treatments to enhance the quality of aluminum alloys to meet industrial-grade wrought aluminum standards. In addition, continued feasibility studies and LCAs should be considered at the production-plant scale.

Use of AI tools declaration

The authors declare they have not used Artificial Intelligence (AI) tools in the creation of this article.

Acknowledgments

This study was supported in part by NEDO (New Energy and Industrial Technology Development Organization) and the National Institute of Advanced Industrial Science and Technology. The research was funded by NEDO with the grant number of JPNP14004. We thank Michio Kobayashi for his contributions to improving the quality of the manuscript.

Conflict of interest

The authors declare no conflict of interest.

Reference

1. Guilhem G, Nicholas P, Bertrand L (2016) Life Cycle Assessment of aluminum recycling process: Case Shredder Cables. *Process CIRP* 48: 212–218. <https://doi.org/10.1016/j.procir.2016.03.097>
2. Paraskevas D, Kellens K, Dewulf W, et al. (2015) Environmental modeling of aluminum recycling: a Life Cycle Assessment tool for sustainable metal management. *J Cleaner Product* 105: 357–370. <https://dx.doi.org/10.1016/j.jclepro.2014.09.102>
3. Nakajima K, Takeda O, Miki T, et al. (2011) Thermodynamic analysis for the controllability of elements in the recycling process of metals. *Environ Sci Technol* 45: 4929–4936. <https://doi.org/10.1021/es104231n>
4. Hatayama H, Daigo I, Matsuno Y, et al. (2012) Evolution of aluminum recycling initiated by the introduction of next-generation vehicles and scrap sorting technology. *Resour Conserv Recycl* 66: 8–14. <https://doi.org/10.1016/j.resconrec.2012.06.006>
5. Kelly SM (2018) Recycling of passenger vehicles: A framework for upcycling and required enabling technologies. PhD Dissertation, April 2018. Worcester Polytechnic Institute.
6. International Aluminum Institute (IAI) (2012) Global Aluminum Recycling: A Cornerstone of Sustainable Development. Available from: <https://www.world-aluminum.org>
7. IDEA_v2.1.3 database (2017) Advanced Industry Science and Technology.
8. AMETEK (2011) Aluminum Recycling -Add Vale by Analysis. Available from: https://spectro.jp/uploads/Aluminum_Recycling_Feb2011_web0.pdf
9. Modaresi R, Müller DB (2012) The role of automobiles for the future aluminum recycling. *Environ Sci Technol* 46: 8587–8594. <https://doi.org/10.1021/es300648w>
10. Global Aluminum Recycling (2009) A cornerstone of sustainable development. http://www.worldaluminium.org/media/filer_public/2013/01/15/f10000181.pdf
11. Kevorkian V (2010) Advances in recycling of wrought aluminum alloys for added value maximisation. *MJM* 16: 103–114. UDC: 669.14:621.791.037
12. Cullen JM, Allwood JM (2013) Mapping the global flow of aluminum: From liquid aluminum to end-user goods. *Environ Sci Technol* 47: 3057–3064. <https://doi.org/10.1021/es304256s>
13. Martinsen K, Gulbrandsen-Dahl S (2015) Use of post-consumer scrap in aluminum wrought alloy structural components for the transportation sector. *Procedia CIRP* 29: 686–691. <https://doi.org/10.1016/j.procir.2015.02.072>
14. McQueen HJ, Spigarelli SS, Kassner ME, et al. (2011) Hot Deformation and Processing of Aluminum Alloys, 1st ed., CRC Press. <https://doi.org/10.1201/b11227>
15. Das SK (2006) Material Science Forum, 519–512: 1239.
16. Kondo M, Maeda H, Mizuguchi M (1990) The production of high-purity aluminum in Japan. *JOM* 42: 36–37. <https://doi.org/10.1007/BF03220434>
17. Mehmetaj B, Bruinsma O, Kool W, et al. (2002) Aluminum scrap recycling with solid layer fractional crystallization. In *15th International Symposium on Industrial Crystallization (ISIC-15)*, Sorrento, Italy, September 15–18.
18. Peel A, Herbert J (2011) Technology for electromagnetic stirring of aluminum reverberatory furnaces. *Light Metals* 2011: 1193–1198.
19. El-Kaddar N, Ashish PD, Natarajan TT (1995) The electromagnetic filtration of molten aluminum using an induced-current separator. *JOM* 47: 46–49. <https://doi.org/10.1007/BF0321176>
20. Park PJ, Tanaka Y, Sassa K, et al. (1994) *International Symposium On Electromagnetic Processing*

of Materials, Nagoya, ISIJ, 497.

21. Zou Q, Tian H, Zhang Z, et al. (2020) Controlling segregation behavior of primary Si in hypereutectic Al-Si alloy by electromagnetic stirring. *Metals* 10: 1129. <https://doi.org/10.3390/met10091129>
22. Kawajiri K, Goto T, Kon Y, et al. (2020) Development of life cycle assessment of an emerging technology at research and development stage: A case study on single-wall carbon nanotube produced by super growth method. *J Clean Prod* 255: 120015. <https://doi.org/10.1016/j.jclepro.2020.120015>
23. Weyand S, Kawajiri K, Mortan C, et al. (2023) Scheme for generating upscaling scenarios of emerging functional materials based energy technologies in prospective LCA (UpFunMatLCA). *J Indust Ecol* 27: 676–692. <https://doi.org/10.1111/jiec.13394>
24. Kawajiri K, Sakamoto K (2022) Environmental impact of carbon fibers fabricated by an innovative manufacturing process on life cycle greenhouse gas emissions. *Sustain Mater Technol* 31: e00365. <https://doi.org/10.1016/j.susmat.2021.e00365>
25. Kawajiri K, Kishita Y, Shinohara Y (2021) Life cycle assessment of thermoelectric generators (TEGs) in an automobile application. *Sustainability* 13: 13630. <https://doi.org/10.3390/su132413630>
26. Lee GC, Kim MG, Park JP, et al. (2010) Iron removal in aluminum melts containing scrap by electromagnetic stirring. *Mater Sci Forum* 638–642: 267–272. <https://doi.org/10.4028/www.scientific.net/MSF.638-642.267>
27. Murakami Y, Omura N (2021) Reduction of Impurity Elements by Applying Electromagnetic Stirring in Fractional Crystallization. In Perander L eds, *Light Metals 2021*, The Minerals, Metals & Materials Series, Springer, Cham, 818–821. https://doi.org/10.1007/978-3-030-65396-5_107
28. Kawajiri K, Inoue T (2016) Cradle-to-gate greenhouse gas impact of nanoscale thin-film solid oxide fuel cells considering scale effect. *J Clean Prod* 112: 4065–4070. <https://doi.org/10.1016/j.jclepro.2015.05.138>